Proceedings of the 9th World Congress on Momentum, Heat and Mass Transfer (MHMT'24)
London, United kingdom – April 11 – 13, 2024
Paper No. ENFHT 268
DOI: 10.11159/enfht24.268

Computational Fluid Dynamics Analysis of Absorber Tube with Molten Salt-based Nanofluids and Porous Medium Inserts

Zhaoping Ying[1], Junfeng Yang[2], Boshu He[3]
[1] Interdisciplinary Center for Scientific Computing, Heidelberg University, Heidelberg, Germany
zhaoping.ying@iwr.uni-heidelberg.de
[2] School of Mechanical Engineering, University of Leeds, Leeds, United Kingdom
J.Yang@leeds.ac.uk
[3] School of Mechanical, Electronic and Control Engineering, Beijing Jiaotong University, Beijing, China
hebs@bjtu.edu.cn

Abstract **-** In the field of solar applications, the performance of the system is significantly influenced by the design of the absorber tube, including the composition of heat transfer fluids within it and its geometric configuration. This study presents a computational fluid dynamics (CFD) model that combines molten salt-based nanofluids with porous medium inserts within the absorber tube. Two distinct configurations of porous inserts are investigated: one attached to the tube wall, referred to as 'enhanced tube 1 (ET1),' and the other integrated into the core zone, denoted as 'enhanced tube 2 (ET2).' This research explores how the thickness of the porous medium in these two configurations impacts the thermal and hydraulic performance of the absorber tube when used with molten salt-based nanofluids. Parameters considered include flow and heat transfer characteristics, as well as a performance evaluation criterion. The thickness of the porous medium is found to play an essential role in the thermo-hydraulic performance of the receiver tube. Across all sizes of ET1, significantly better heat transfer performance is consistently observed when compared to all ET2 configurations. It is important to note that the introduction of porous inserts does result in an increase in pressure drop, which varies with the thickness of the inserts in both ET1 and ET2 configurations. Consequently, when evaluating the overall thermo-hydraulic performance, the ranking stands as ET1 > smooth tube > ET2. Additionally, the performance evaluation criterion of ET1 exhibits an initial increase, followed by a subsequent decrease as the thickness of the porous inserts varies. This pattern suggests the presence of an optimal thickness, with a radius of 0.1, that maximizes performance. This study might contribute to the performance improvement of the absorber tube used in solar applications.

***Keywords*:** Porous medium inserts; Molten salt-based nanofluids; Computational fluid dynamics; Thermo-hydraulic analyses; Absorber tube; Solar energy

1. Introduction

In the realm of solar applications, the performance of the system is notably influenced by the absorber tubes, encompassing not only the geometry but also the heat transfer fluids circulating within them [1-2]. Recent interest has surged in harnessing molten salt-based nanofluids as heat transfer agents within absorbers [3] due to their remarkable heat transfer capabilities [4-5]. Experimental studies by Chen et al. [3] and numerical investigations conducted by Ying et al. [4] and Kaood et al. [5] all consistently report a significant enhancement in thermal performance when utilizing molten salt-based nanofluids for convection within absorbers, as opposed to conventional pure molten salt.

The combination of nanofluids and porous medium inserts holds significant promise for enhancing thermal performance, as supported by several studies [6-11]. El-Shorbagy et al. [6] demonstrated that optimal heat transfer in partially filled trapezoidal channels with porous media occurs when the aspect ratio is set at 0.3, and 90% of the channel is filled with porous material. Wang et al. [7] conducted a numerical investigation involving twisted porous tape and nanofluids in tubes, revealing substantial efficiency and heat exchange improvements when employing porous twisted tape, nanofluids, and triangular tubes. Experimental evidence supports the effectiveness of incorporating porous medium inserts, both inside [8] and outside [9] the absorber, in enhancing heat transfer. However, numerical studies in this regard remain limited. Siavashi et al. [10] concluded that the inclusion of nanoparticles in nanofluids enhances the thermal efficiency of parabolic trough solar collectors. Ying et al. [11] explored the synergistic benefits of combining porous medium and nanofluids to improve the thermo-hydraulic performance of solar collector absorber tubes. Notably, the crucial factor of porous insert thickness, a globally optimized combination condition, remains largely unaddressed.

Therefore, this study employs a Computational Fluid Dynamics (CFD) model to investigate the behavior of molten salt-based nanofluids within the absorber, considering the influence of porous insert thickness on flow and heat transfer characteristics, along with a performance evaluation criterion. The findings of this study offer valuable insights for enhancing the thermo-hydraulic performance of absorber tubes utilized in solar applications.

2. CFD model

2.1. Geometry and parameters

The geometry and flow conditions are the same as those in our former study [11], except for the thickness of the porous inserts inside the tube, cf. the '*d*' in Fig. 1(a). The tube has a radius of 0.008 m and a length of 1 m [12]. Two configurations of porous inserts are considered which are wall attached type labeled as enhanced tube 1 (ET1) and core zone type labeled as enhanced tube 2 (ET2), as illustrated in Fig.1(b).

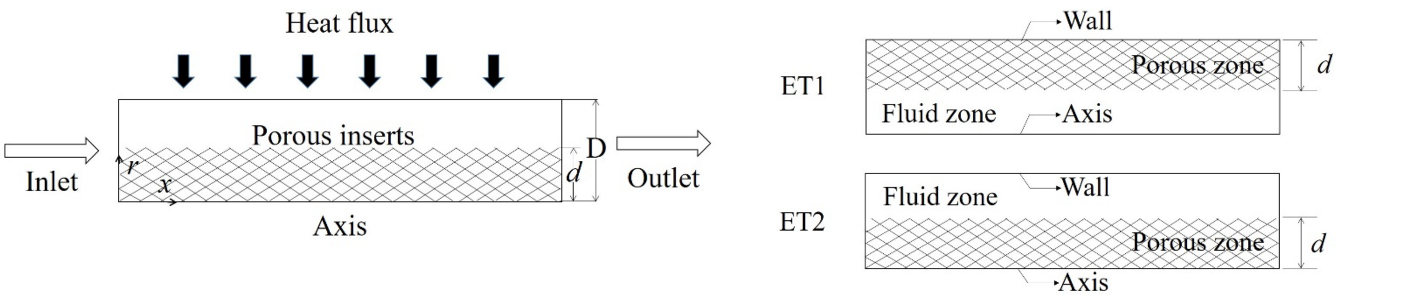

(a) Absorber tube with porous inserts (b) Wall attached type (ET1) and core zone type (ET2)

Figure.1 Schematic diagram of molten salt-based nanofluids inside the tube with two types of porous inserts

2.2. Governing equations

The convective heat transfer behaviors of the molten salt-based nanofluids are described by equations of continuity, momentum, energy, and turbulence model. The governing equations are presented in the cylindrical coordinate. Momentum and energy equations are independent in the fluid zone and porous zone inside the enhanced tube, cf. Fig. 1(b). The fluid flow and heat transfer inside the tube are assumed as steady-state. The contact thermal resistance in the interface of the wall and metal foam is ignored, and the energy transition between the fluid and porous zone is in local thermal equilibrium.

The conservation of mass in the fluid zone and the porous zone is the same form written as Eq. (1):

$$\frac{\partial(\rho_{\mathrm{nf}}u)}{\partial x}+\frac{1}{r}\frac{\partial}{\partial r}(r\rho_{\mathrm{nf}}v)=0 \tag{1}$$

Momentum equations in the fluid and porous region are given as Eqs. (2) and (3) [13], respectively:

$$\begin{aligned}\frac{\partial(\rho_{\mathrm{nf}}uu)}{\partial x}+\frac{1}{r}\frac{\partial}{\partial r}(r\rho_{\mathrm{nf}}uv)&=-\frac{\partial p}{\partial x}+\frac{\partial}{\partial x}\left(\mu_{\mathrm{nf}}\frac{\partial u}{\partial x}\right)+\frac{1}{r}\frac{\partial}{\partial r}\left(r\mu_{\mathrm{nf}}\frac{\partial u}{\partial r}\right)\\ \frac{\partial(\rho_{\mathrm{nf}}uv)}{\partial x}+\frac{1}{r}\frac{\partial}{\partial r}(r\rho_{\mathrm{nf}}vv)&=-\frac{\partial p}{\partial r}+\frac{\partial}{\partial x}\left(\mu_{\mathrm{nf}}\frac{\partial v}{\partial x}\right)+\frac{1}{r}\frac{\partial}{\partial r}\left(r\mu_{\mathrm{nf}}\frac{\partial v}{\partial r}\right)\end{aligned} \tag{2}$$

$$\begin{aligned}\frac{1}{\varepsilon^2}\frac{\partial(\rho_{\mathrm{nf}}uu)}{\partial x}+\frac{1}{r\varepsilon^2}\frac{\partial(r\rho_{\mathrm{nf}}vu)}{\partial r}&=-\frac{\partial p}{\partial x}+\frac{1}{\varepsilon}\frac{\partial\left(\mu_{\mathrm{nf}}\frac{\partial u}{\partial x}\right)}{\partial x}+\frac{1}{r\varepsilon}\frac{\partial\left(r\mu_{\mathrm{nf}}\frac{\partial u}{\partial r}\right)}{\partial r}-\frac{\rho_{\mathrm{nf}}C_d\sqrt{u^2+v^2}u}{\sqrt{K}}-\frac{\mu_{\mathrm{nf}}u}{K}\\ \frac{1}{\varepsilon^2}\frac{\partial(\rho_{\mathrm{nf}}uv)}{\partial x}+\frac{1}{r\varepsilon^2}\frac{\partial(r\rho_{\mathrm{nf}}vv)}{\partial r}&=-\frac{\partial p}{\partial r}+\frac{1}{\varepsilon}\frac{\partial\left(\mu_{\mathrm{nf}}\frac{\partial v}{\partial x}\right)}{\partial x}+\frac{1}{r\varepsilon}\frac{\partial\left(r\mu_{\mathrm{nf}}\frac{\partial v}{\partial r}\right)}{\partial r}-\frac{\rho_{\mathrm{nf}}C_d\sqrt{u^2+v^2}v}{\sqrt{K}}-\frac{\mu_{\mathrm{nf}}v}{K}\end{aligned} \tag{3}$$

Energy equations in the fluid and porous region are presented in Eqs. (4) and (5) [14] (Bozorg et al. 2020), respectively:

$$\frac{\partial}{\partial x}\left(\rho_{\mathrm{nf}} u c_{\mathrm{p,nf}} T\right)+\frac{1}{r}\frac{\partial}{\partial r}\left(r\rho_{\mathrm{nf}} v c_{\mathrm{p,nf}} T\right)=\frac{\partial}{\partial x}\left(k_{\mathrm{nf}}\frac{\partial T}{\partial x}\right)+\frac{1}{r}\frac{\partial}{\partial r}\left(r k_{\mathrm{nf}}\frac{\partial T}{\partial r}\right) \tag{4}$$

$$\frac{\partial}{\partial x}\left(\rho_{\mathrm{nf}} u c_{\mathrm{p,nf}} T\right)+\frac{1}{r}\frac{\partial}{\partial r}\left(r\rho_{\mathrm{nf}} v c_{\mathrm{p,nf}} T\right)=\frac{\partial}{\partial x}\left(k_{\mathrm{eff}}\frac{\partial T}{\partial x}\right)+\frac{1}{r}\frac{\partial}{\partial r}\left(r k_{\mathrm{eff}}\frac{\partial T}{\partial r}\right) \tag{5}$$

Each variable's physical significance can be readily discerned through the nomenclature detailed in the Appendix. Turbulence inside the tube is modeled with the standard k-ε model [15] (Launder and Spalding, 1972) with enhanced wall treatment in the simulation [11]. The thermophysical properties of molten salt (HITEC), molten salt-based Al_2O_3 nanofluids and materials of the porous medium can be found in the former study [4, 11]. Comprehensive information regarding the initial and boundary conditions, numerical configurations, and a thorough validation process can be found in reference [11].

3. Results and discussion

The CFD model is employed to study the impact of varying thicknesses of porous inserts on the thermo-hydraulic performance of molten salt-based nanofluids flowing within the absorber tube equipped with porous inserts. While the idea of enhancing heat transfer in the core flow (which is the ET2 type considered in our research) had been studied and proven in some researches [13, 16], the thermal-hydraulic performance of ET2 was not as good as that of ET1 [11, 16]. The effect of the porous radius ratio, *rad* = *d*/D (D is the radius of the tube), of ET1 and ET2 on the thermo-hydraulic performance of receiver tubes with molten salt-based nanofluids is further parametrically studied. To provide a more comprehensive assessment of the combined technique's thermo-hydraulic performance, a performance evaluation criterion ($PEC = (Nu/Nu_{\mathrm{s}})/(f/f_{\mathrm{s}})^{1/3}$) is used, where the subscript $'s'$ stands for the smooth tube in which pure HITEC flows and no porous metal foam is inserted. The ET1 and ET2 are inserted with copper metal foam (porosity is 0.9005), and the concentration of molten salt-based nanofluids is 0.125 wt% (mass fraction) and the *Re* number is 1×10^4.

The thickness of the porous medium significantly influences the thermo-hydraulic performance of the receiver tube, as depicted in Fig. 2. From these figures, it is evident that the values of Nu/Nu_{s} of ET1 are considerably higher than those of ET2, signifying that the heat transfer performance of ET1 surpasses that of ET2. In Fig. 2(a), the Nu/Nu_{s} values for ET2 slightly exceed unity, suggesting that the introduction of porous medium enhances the heat transfer performance of the receiver tube. From Fig. 2(b), it is evident that the penalty of pressure drop increases with the thickness of the porous inserts increases in both ET1 and ET2. Additionally, Fig. 2(c) reveals that the *PEC* values of ET1 are greater than unity, while those of ET2 are not. This suggests that the thermo-hydraulic performance order is ET1 > smooth tube > ET2. Notably, the heat transfer and thermo-hydraulic performance of ET1 initially rise and then decline with increasing thickness of the porous inserts. Therefore, an optimum thickness for the porous inserts exists between 0 and 0.2.

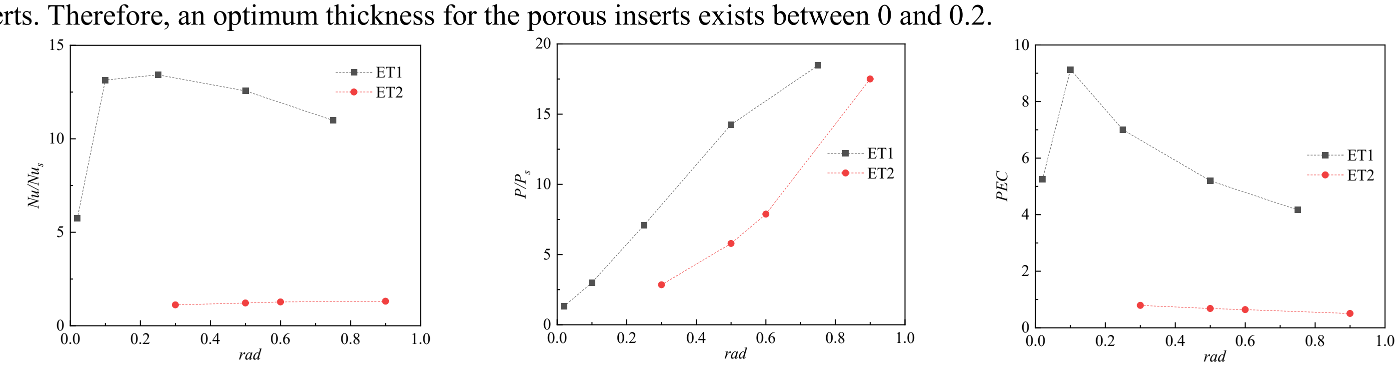

(a) Nu/Nu_{s} (b) $P_{\mathrm{p}}/P_{\mathrm{p,\,s}}$ (c) *PEC*

Figure. 2 Comparisons of the different radius of ET1 and ET2

4. Conclusion

A computational fluid dynamics (CFD) model is employed to simulate the thermo-hydraulic performance of molten salt-based nanofluids with porous medium inserts inside the absorber tube. Two configurations of porous inserts are considered, and the influence of porous medium thickness on the thermo-hydraulic performance is thoroughly examined. Molten salt-based nanofluids exhibit a considerable heat transfer performance when flowing inside the tube with a porous medium, outperforming pure molten salt in a smooth tube. The ET1 tube configuration consistently outperforms other configurations, and it maintains superior performance across all ET1 sizes when compared to all ET2 configurations. However, it's worth noting that the pressure drop penalty increases with greater thickness of the porous inserts in both ET1 and ET2 configurations. Consequently, after evaluating the performance criteria, the overall thermos-hydraulic performance ranking stands as ET1 > smooth tube > ET2. The performance evaluation criterion study of ET1 indicates the presence of an optimal value with a radius of 0.1.

References

[1] I. F. Okafor, J. Dirker, J. P. Meyer, "Influence of circumferential solar heat flux distribution on the heat transfer coefficients of linear Fresnel collector absorber tubes," *Sol. Energy*, vol. 107, pp. 381-397, 2014.

[2] K. Skrbek, V. Bartůněk, D. Sedmidubsky, "Molten salt-based nanocomposites for thermal energy storage: Materials, preparation techniques and properties," *Renew. Sust. Energ. Rev.*, vol. 164, pp. 112548, 2022.

[3] H. Chen, X. Chen, Y. Wu, Y. Lu, X, Wang, C. Ma, "Experimental study on forced convection heat transfer of KNO_3-$Ca(NO_3)_2$+SiO_2 molten salt nanofluid in circular tube," *Sol. Energy*, vol. 206, pp. 900-906, 2020.

[4] Z. Ying, B. He, L. Su, Y. Kuang, D. He, C. Lin, "Convective heat transfer of molten salt-based nanofluid in a receiver tube with non-uniform heat flux," *Appl. Therm. Eng.*, vol. 181, pp. 115922, 2020.

[5] A. Kaood, M. Abubakr, O. Al-Oran, M. A. Hassan, "Performance analysis and particle swarm optimization of molten salt-based nanofluids in parabolic trough concentrators," *Renew. Energ.*, vol. 177, pp. 1045-1062, 2021.

[6] Y. Wang, C. Qi, Z. Ding, J. Tu, R. Zhao, "Numerical simulation of flow and heat transfer characteristics of nanofluids in built-in porous twisted tape tube," *Powder Technol.*, vol. 392, pp. 570-586, 2021.

[7] M. A. El-Shorbagy, F. Eslami, M. Ibrahim, P. Barnoon, W. Xia, D. Toghraie, "Numerical investigation of mixed convection of nanofluid flow in a trapezoidal channel with different aspect ratios in the presence of porous medium", *Case Stud. Therm. Eng.*, vol. 25, pp. 100977, 2021.

[8] H. Ebadi, A. Cammi, R. Difonzo, J. Rodríguez, L. Savoldi, "Experimental investigation on an air tubular absorber enhanced with raschig rings porous medium in a solar furnace," *Appl. Energy*, vol. 342, pp. 121189, 2023.

[9] N. F. Jouybari and T. S. Lundstrom, "Performance improvement of a solar air heater by covering the absorber plate with a thin porous material" *Energy*, vol. 190, pp. 116437, 2020.

[10] M. Siavashi, M. B. Vahabzadeh, M. H. Toosi, "A numerical analysis of the effects of nanofluid and porous media utilization on the performance of parabolic trough solar collectors," *Sustain. Energy Technol. Assess.* Vol. 45, pp. 101179, 2021.

[11] Z. Ying, B. He, L. Su, Y. Kuang, "Thermo-hydraulic analyses of the absorber tube with molten salt-based nanofluid and porous medium inserts," *Sol Energy*, vol. 226, pp. 20-30, 2021.

[12] X. Yang, X. Yang, J. Ding, Y. Shao, H. Fan, "Numerical simulation study on the heat transfer characteristics of the tube receiver of the solar thermal power tower," *Appl. Energy*, Vol. 90, No. 1, pp. 142-147, 2012.

[13] Z. Huang, A. Nakayama, K. Yang, C. Yang, W. Liu, "Enhancing heat transfer in the core flow by using porous medium insert in a tube," *Int. J. Heat Mass Transf.*, Vol. 53, No. 5–6, pp. 1164-1174, 2010.

[14] M. V. Bozorg, M. H. Doranehgard, K. Hong, Q. Xiong, "CFD study of heat transfer and fluid flow in a parabolic trough solar receiver with internal annular porous structure and synthetic oil–Al_2O_3 nanofluid," *Renew. Energy*, Vol. 145, pp. 2598-2614, 2020.

[15] B. E. Launder, D. B. Spalding, *Lectures in mathematical models of turbulence*. London, Academic Press, 1972.

[16] Z. Zheng, M. Li, Y. He, "Thermal analysis of solar central receiver tube with porous inserts and non-uniform heat flux," *Appl. Energy*, Vol. 185, pp. 1152-1161, 2017.

Appendix

Nomenclature

c_p	Specific heat capacity, [J/kg·K]	T	Temperature, [K]
d	Thickness of metal foam, [m]	u/v	Axial/radical velocity, [m/s]
D	Tube diameter, [m]	wt%	Mass fraction, [%]
ET	Enhanced tube	x	Axial distance, [m]
f	Friction factor	y^+	Dimensionless wall distance
C_d	Inertia coefficient	Greek Letters	
HITEC	KNO_3, $NaNO_2$ and $NaNO_3$	μ	Dynamic viscosity, [kg/m·s]
k	Thermal conductivity, [W/m·K]	ρ	Density, [kg/m^3]
K	Permeability, [m^2]	Subscripts	
Nu	Nusselt number	eff	Effective
P	Static pressure, [N/m^2]	nf	Nanofluid
PEC	Performance evaluation criterion	s	Smooth tube
Re	Reynolds number		